

Protection of excited spin states by a superconducting energy gap

B. W. Heinrich^{1*}, L. Braun^{1†}, J. I. Pascual^{1,2,3} and K. J. Franke¹

The latest concepts for quantum computing and data storage rely on the addressing and manipulation of single spins. A limitation for single atoms or molecules in contact with a metal surface is the short lifetime of excited spin states, typically picoseconds, due to the exchange of energy and angular momentum with the itinerant electrons of the substrate^{1–4}. Here we show that paramagnetic molecules on a superconducting substrate exhibit excited spin states with a lifetime of $\tau \approx 10$ ns. We ascribe this increase in lifetime by orders of magnitude to the depletion of electronic states around the Fermi level in the superconductor. This prohibits pathways of energy relaxation into the substrate and allows the magnetic molecule to be electrically pumped into higher spin states, making superconducting substrates prime candidates for spin manipulation. We further show that the proximity of the scanning tunnelling microscope tip modifies the magnetic anisotropy.

The most efficient method for energy quenching on metallic substrates is the creation of electron–hole pairs⁵. A common strategy to decouple spin states from their electronic environment is to include a non-conductive spacer^{3,6,7}, with an energy gap in the density of states (DoS) at the Fermi level (E_F). Superconductors exhibit a small but perfect energy gap around the Fermi level owing to the condensation of electrons into Cooper pairs at low temperatures. As the energy scales of superconducting pairing and spin excitations are typically similar, superconductors are ideal materials for stabilizing excited spin states, combining a perfect gap in the DoS at E_F with normal metal conductivity, which still allows the spin to be addressed by means of conducting leads.

However, magnetism and superconductivity do not easily coexist. Exchange interaction of a magnetic species with Cooper pairs affects the superconducting ground state and gives rise to new states within the energy gap^{8–11}. To overcome the exchange coupling to the superconductor, our study focuses on paramagnetic metal–organic molecules, whose molecular ligand with inert organic groups separates the central magnetic ion from its conducting environment. At the same time, the organic skeleton provides an anisotropic environment⁷, leading to non-degenerate magnetic eigenstates in the absence of an external magnetic field¹². We study Fe–octaethylporphyrin–chloride (Fe–OEP–Cl; structure as in Fig. 1b) adsorbed on Pb(111), whose Fe centre has, in gas phase¹³ and bulk¹⁴, a +3 oxidation state with a spin of $S = 5/2$ and an in-plane anisotropy (anisotropy parameter $D > 0$).

To address the dynamics of excited spin states of Fe–OEP–Cl on a superconducting Pb substrate, we use a scanning tunnelling microscope (STM) at a temperature of 1.2 K with a Pb-covered tip (Methods for details). In the differential conductance [$dI/dV(V)$]

spectra on the bare Pb(111) substrate, the depletion of the density of states around E_F is reflected by a gap terminated by two sharp quasi-particle [Bardeen–Cooper–Schrieffer (BCS)] peaks at $|eV| = \Delta_{\text{tip}} + \Delta_{\text{sample}} = 2\Delta = 2.7$ meV, that is, twice the superconducting gap (Fig. 1c, bottom; Δ_{tip} (Δ_{sample}) is the superconducting gap parameter of the tip (sample), e the elementary charge).

Fe–OEP–Cl self-assembles on the Pb(111) surface in large quasi-hexagonal molecular islands (Fig. 1a). STM images show that many molecules have lost their Cl ligand during deposition¹⁵. To characterize the spin state of Fe–OEP–Cl, $dI/dV(V)$ spectra were acquired at the centre, on top of the Cl ligand (Fig. 1c). The energy gap and quasi-particle resonances of the Pb substrate are observed unchanged on the Fe–OEP–Cl molecules, revealing that the superconducting state is unaffected by the presence of the paramagnetic molecule. We thus conclude that, owing to the decoupling ligand, no noticeable magnetic interaction of the molecular spin with the superconductor occurs.

The presence of the paramagnetic molecule causes, instead, remarkable peak features outside the superconducting gap. They are symmetric with respect to E_F , indicating an origin related to inelastic electron tunnelling phenomena^{6,16,17}. In normal metal tunnelling junctions, the opening of an inelastic tunnelling channel due to a molecular excitation produces a step-wise increase of the differential conductance at the excitation energy ε . Here, the effect of the superconducting DoS of the tip and sample is twofold: first, it causes a shift of 2Δ in the energy of the inelastic onsets, which appear now at $|eV| = 2\Delta + \varepsilon$, and second, it induces a repetition of the BCS peaks at this excitation threshold owing to the peaked DoS (Fig. 1d). The energy of the inelastic excitation in the spectra of Fig. 1c is $\varepsilon_1 = 1.4$ meV and the relative amplitude with respect to the BCS peaks is ≈ 0.4 . These values are typical for spin excitations of paramagnetic species in the presence of ligand field anisotropy^{7,18,19}. The inelastic tunnelling occurs when electrons exchange energy and angular momentum of $\Delta M_S = \pm 1, 0$ (refs 18,19)— M_S are the spin eigenstates—with the spin of the Fe^{3+} centre and induce the non-equilibrium population of excited states in the spin multiplet.

A careful analysis of the excitation spectra of Fe–OEP–Cl reveals signatures of a second excitation at an energy $\varepsilon_2 = 2.8$ meV, that is, at $2 \times \varepsilon_1$ (dashed circle in Fig. 1c). From these two excitations we deduce the $S = 5/2$ spin state of the Fe–OEP–Cl molecule. Only this multiplet of Fe^{3+} splits in the presence of axial magnetic anisotropy into three doublets: $M_S = \pm 1/2$; $\pm 3/2$; and $\pm 5/2$ (Fig. 2b), separated by energies of $2D$ and $4D$ (ref. 12). The observation of two inelastic excitations with $\varepsilon_2 = 2 \times \varepsilon_1$ is possible only if the Kramer doublet with $M_S = \pm 1/2$ is the ground state of

¹Institut für Experimentalphysik, Freie Universität Berlin, Arnimallee 14, 14195 Berlin, Germany, ²CIC nanoGUNE, 20018 Donostia-San Sebastián, Spain, ³Ikerbasque, Basque Foundation for Science, 48011 Bilbao, Spain. [†]Present address: Fritz-Haber-Institut der Max-Planck-Gesellschaft, 14195 Berlin, Germany. *e-mail: bheinrich@physik.fu-berlin.de

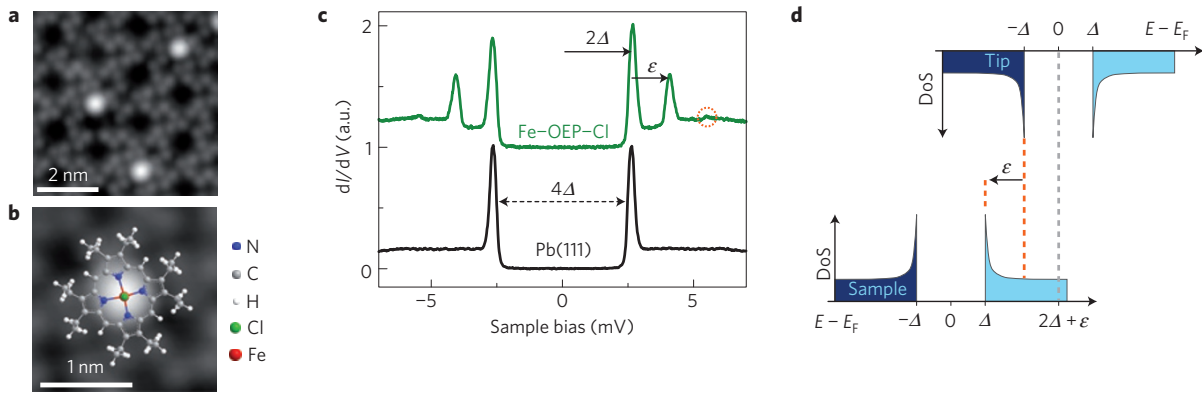


Figure 1 | Fe-OEP-Cl on Pb(111). **a**, STM topography of a mixed island of Fe-OEP-Cl (molecules with a bright protrusion) and Fe-OEP (molecules with a dark centre; scanning conditions: $V = -50$ mV, $I = 200$ pA). **b**, Zoom on a single Fe-OEP-Cl with superimposed molecular structure. **c**, $dI/dV(V)$ spectra acquired above pristine Pb(111) and Fe-OEP-Cl (feedback loop opened at $I = 200$ pA and $V = 50$ mV followed by an approach $\Delta z = -110$ and 0 pm, respectively; spectra normalized to unity at the energy of the quasi-particle peaks and offset for clarity). The quasi-particle peaks at $|eV| = 2\Delta$ indicate an unperturbed superconducting state. A pair of strong peaks and weak peaks (marked by a dashed circle) in the $dI/dV(V)$ on the molecule are signatures of inelastic tunnelling in a superconductor–vacuum–superconductor junction, as sketched in **d**: peaks appear at energies $|eV| = 2\Delta + \varepsilon$ as a result of the opening of an inelastic tunnelling channel.

the multiplet (as will be presented in the following). The resulting in-plane magnetic anisotropy with $D = 0.7$ meV is in sign and magnitude similar to the known values for Fe-OEP-Cl in bulk samples¹⁴, indicating again the minor interaction between the molecular spin and the Pb(111) substrate.

Although a spin $S = 5/2$ allows two zero field excitations with $\Delta M_S = \pm 1$, the higher-energy excitation ($\pm 3/2 \rightarrow \pm 5/2$) is possible only if the intermediate state $M_S = \pm 3/2$ is populated with a finite probability. At the low temperature of our experiment, the thermal occupation of the intermediate state is negligible, but it can be populated through preceding inelastic tunnelling events. In fact, we observe that the second excitation emerges in the spectra when the tip is brought closer and larger tunnelling currents are applied (Fig. 2a), which is a fingerprint of spin pumping into higher-lying excited states⁵.

To monitor how the tunnelling current enables the population of excited spin states, in Fig. 2c we plot the current dependence of the relative amplitude of the two inelastic peaks, A_{r1} and A_{r2} (Methods). An asymptotic increase of the relative amplitudes with the current is observed for both excitations. For the first excitation, A_{r1} increases by about 20% and saturates for currents larger than 0.6×10^9 electrons per second (≈ 0.1 nA). The second excitation is hardly detectable at low tunnelling current values, but, when it appears, A_{r2} increases rapidly with the current I . For the smallest current values, the mean time between tunnelling electrons is much larger than the excitation lifetime τ_1 . Spin excitation from the ground state to state 1 is the only possible inelastic event. The pronounced increase of both inelastic signals with current indicates the activation of further inelastic processes due to long spin excitation lifetimes. When the inelastic tunnelling rate equals the natural decay constant of this excitation $\lambda_1 = 1/\tau_1$, tunnelling electrons may find the molecule still populating state 1 and contribute to the spin relaxation by absorbing the excitation energy. This inelastic decay channel is open to all electrons and, hence, causes an increase of A_{r1} . The saturation of A_{r1} for currents above 0.1 nA denotes a stationary non-equilibrium state, with transitions between the ground and first excited spin state being solely driven by the inelastic current. A consequence of this is a finite population of the first excited state (state 1), which then enables excitations to the second excited state⁵ (state 2). This is reflected in the appearance of the inelastic signal at $\varepsilon_2 = 2 \times \varepsilon_1$. This scenario corroborates our earlier assignment of $M_S = \pm 1/2$ being the ground state, that is, $D > 0$.

To obtain a precise value for the natural lifetime $\tau_1 = 1/\lambda_1$ of state 1 ($|M_S| = 3/2$), we set up rate equations accounting for changes of the ground and excited state occupation (N_0 and N_1). The excitation process is driven by tunnelling electrons above the threshold energy $eV \geq 2\Delta + \varepsilon_1$, and depends on the inelastic transition probability P and on the elastic current through the BCS peak I_{BCS} (a detailed explanation is included in the Supplementary Information). The relaxation process contains, besides the spontaneous decay with constant λ_1 , an electron-induced inelastic de-excitation. As the timescale of our experiment is long compared to the tunnelling frequency, we measure a stationary state of the occupations N_0 and N_1 , which depends on the tunnelling current. From the rate equations (Supplementary Information), we obtain that the relative amplitude A_{r1} depends on the elastic current I_{BCS} as:

$$A_{r1} = P \frac{(I_{BCS}/e)P(2 + 2\varepsilon_1/\Delta) + \lambda_1}{(I_{BCS}/e)P(2 + \varepsilon_1/\Delta) + \lambda_1} \quad (1)$$

We use equation (1) to fit the dependence of A_{r1} with current in Fig. 2c and obtain that the lifetime of the first excited state is $\tau_1 = 1/\lambda_1 = 12 \pm 3$ ns, in agreement with the appearance of the second excitation peak for currents on the order of $10^8 e/s$. This value is larger by orders of magnitude than typical spin excitation lifetimes of magnetic atoms on metal substrates, where τ typically spans up to a few hundred femtoseconds^{1,2,20}. Furthermore, it is still larger by more than one order of magnitude than the lifetime of single atoms on top of thin decoupling layers such as CuO, BN or Cu₂N (refs 3,5,7), which succeeded in extending spin lifetimes up to hundreds of picoseconds.

For currents larger than 0.1 nA, the population of the $M_S = \pm 3/2$ state increases to about 30% (Supplementary Fig. 6), allowing tunnelling electrons to excite a second transition to the $M_S = \pm 5/2$ state (state 2) when their energy reaches the $4D$ threshold value (≈ 2.8 meV). The increase of the relative amplitude A_{r2} from zero to ~ 0.12 with current is essentially a consequence of the increase of the population of the intermediate state 1, which enables the second excitation and corresponds roughly to the product of the stationary, non-equilibrium population of state 1 times the transition probability P . The fit of A_{r2} as described in the Supplementary Information confirms the lifetime τ_1 being of the order of 10 ns. It further hints at a lifetime τ_2 being significantly shorter than τ_1 .

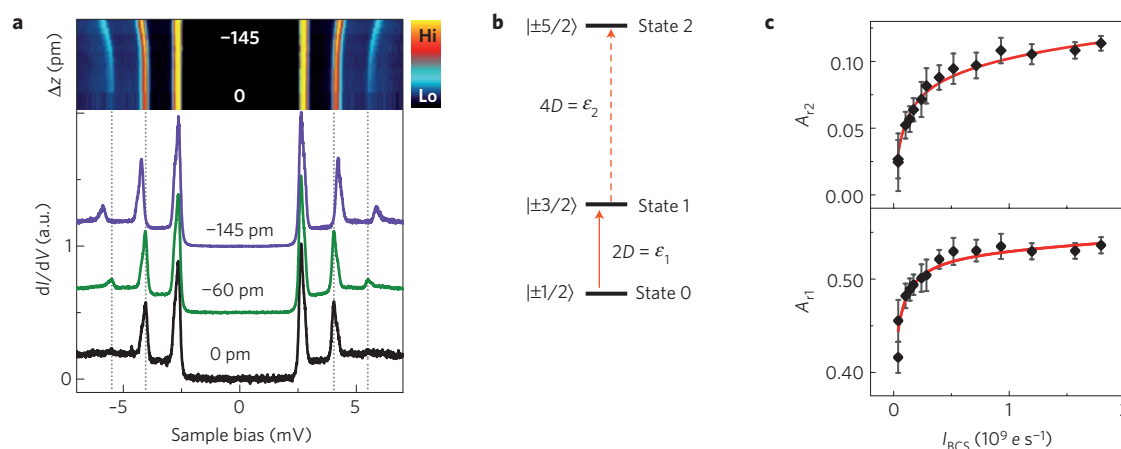


Figure 2 | Long lived excited spin states probed by distance-dependent excitation spectra. **a**, dI/dV spectra acquired at different tip-sample distances reveal: the intensity of both inelastic excitations increases, and the excitation energies shift to higher energies with decreasing distance. The top panel shows a 2D intensity plot of a series of distance-dependent dI/dV spectra. All spectra are normalized to unity at the energy of the quasi-particle peaks and offset for clarity ($I = 200$ pA, $V = 50$ mV; Δz ranging from 0 to -145 pm). **b**, Scheme of the zero-field-splitting (ZFS) for $S = 5/2$ with in-plane anisotropy ($D > 0$). Owing to conservation of angular momentum, a tunnelling electron can change the spin state only by $\Delta M_S = \pm 1$ or 0 (refs 18,19). **c**, Relative amplitude A_{11} (A_{12}) of the first (second) excitation resonance as a function of I_{BCS} , the current integral of the BCS peaks. The error bars are determined via error propagation from the uncertainties of the respective amplitudes. The lifetime of the excited state is fitted to the asymptotic increase, as described in the text (red line; fit parameters for A_{11} : $\tau_1 = 12 \pm 3$ ns; $P = 0.39 \pm 0.02$). For A_{12} , the fit is described in the Supplementary Information ($\tau_1 = 12.3$ ns; $\tau_{2 \rightarrow 0} = 100$ ns; free fit parameters: $\tau_{2 \rightarrow 1} = 400 \pm 100$ ps; $P = 0.25 \pm 0.02$; $\chi^2 = 0.16$.)

To explain the long lifetime of state 1, we note that the most efficient spin relaxation channel on metal surfaces consists of spin scattering with conduction electrons and the creation of electron-hole pairs. On the Pb surface, the superconducting energy gap around E_F amounts to $2\Delta = 2.7$ meV; which is larger than the energy of the first excited state $\varepsilon_1 = 1.4$ meV. Hence, absorption of the spin excitation energy by electron-hole-pair creation is blocked. The absence of the most efficient relaxation channel extends the state's lifetime. Only other less efficient relaxation channels, such as direct and indirect spin-phonon coupling, can release energy by excitations in the phonon band of the substrate²¹. The importance of the energy gap of the substrate is further reflected by the hint that the lifetime of the second excited state is considerably shorter. For this excitation $\varepsilon_2 > 2\Delta$ and it can thus decay directly into the substrate by electron-hole-pair excitations. Such a fast excitation decay would also be the case for the first excited state if Fe-OEP-Cl were not adsorbed on superconducting Pb(111), but on a normal metal substrate with similar adsorption properties, such as Au(111) (Supplementary Section V). On Au(111) no sign of a second excitation is observed for Fe-OEP-Cl, allowing us to determine an upper limit of 400 ps for the lifetime of τ_1 . This finding underlines the importance of the superconducting state for the protection of the excited spin state 1.

A remarkable effect observed in Fig. 2 is the monotonous increase of both spin excitation energies with a decrease in tip-sample distance. Figure 3 shows that the inelastic onsets ε_1 and ε_2 grow exponentially with displacement of the tip, while their ratio amounts to $\varepsilon_1/\varepsilon_2 = 2$ at every tip position. The constant ratio of two indicates that the energy shifts are caused by the continuous increase of the anisotropy D as the STM tip approaches the Cl ion, owing to an exponentially increasing wave function overlap. D amounts to 0.70 ± 0.01 meV at the limit of zero current, that is, in the absence of the tip, and increases to 0.80 ± 0.02 meV at the closest possible position. The gradual increase of $\approx 15\%$ in the magnetic anisotropy is induced by the proximity of the STM tip to the paramagnetic species and is probably a consequence of the forces exerted on the molecule, which scale exponentially with the tip-molecule distance²². Before the forces become too strong and the chlorine ion is detached, mechanical deformations of the molecule lead to a change in the

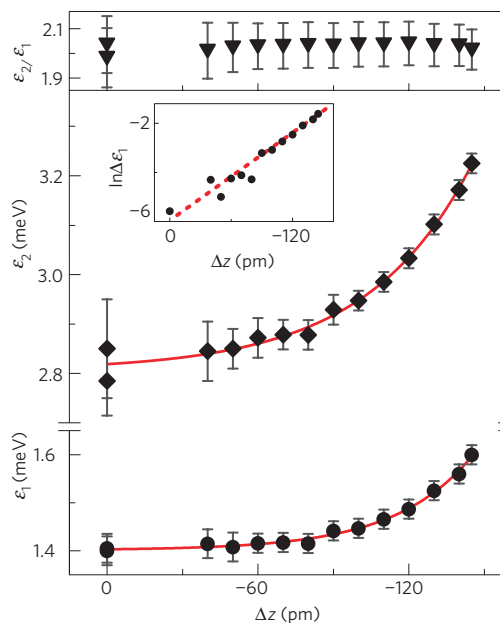


Figure 3 | Changing the magnetic anisotropy with the STM tip. The excitation energies of the first (bottom) and second (middle) excitation, and their ratio $\varepsilon_1/\varepsilon_2$ are drawn as a function of the relative tip-sample distance Δz . The error bars are determined from the error in the measurements of the respective peak positions. An exponential fit yields zero-current excitation energies of $\varepsilon_1^0 = 1.40 \pm 0.01$ meV, and $\varepsilon_2^0 = 2.81 \pm 0.01$ meV. The linear slope in the logarithmic plot (see inset) of the excitation energy difference $\Delta \varepsilon_1 = \varepsilon_1(\Delta z) - \varepsilon_1^0$ reveals the influence of the increased wavefunction overlap of tip and molecule on the magnetic anisotropy (dashed line is a guide for the eye).

crystal field of the Fe^{3+} core and, hence, its magnetic anisotropy. This effect exemplifies the tunability of anisotropy of single atoms by reversible changes in their atomic-scale surroundings²³, with the changes being strongest in rather flexible environments such as coordinatively bonded metal-organic complexes.

Traditionally, atomic magnetism uses semiconducting substrates or insulating layers to extend magnetic excitation lifetimes to levels that allow the manipulation of spins. Our results show that the combination of a passive organic ligand and a superconducting substrate preserve magnetic states and spin excitations from decaying for several nanoseconds. This timescale would be long enough for quantum information processing in multi-centre molecular magnets²⁴, and for electrical spin pumping and reading⁵.

Methods

Our experiments were carried out in a SPECS JT-STM, an ultra-high vacuum scanning tunnelling microscope operating at a base temperature of 1.2 K. Spectra of the differential conductance $dI/dV(V)$ were acquired under open-feedback conditions with a standard lock-in technique using a modulation frequency of $f = 912$ Hz and an amplitude of $V_{\text{rms}} = 30\text{--}50\ \mu\text{V}$. The Pb(111) surface (critical temperature $T_c = 7.2$ K) was cleaned by repeated sputter/anneal cycles until a clean, superconducting surface was obtained. The Pb tip was prepared by indenting the tip into the Pb surface while applying a voltage of 100 V. To check the quality of the as-prepared tips we record dI/dV spectra on the bare Pb(111) surface at 4.8 K. At this temperature, thermal excitations of the quasi-particles across the superconducting energy gap lead to a finite number of hole-like states at $-\Delta$ and electron-like states at $+\Delta$. If the superconducting gaps of tip and sample are of the same width, that is, $\Delta_{\text{tip}} = \Delta_{\text{sample}}$, this finite state occupation results in a small conductance peak exactly at zero bias¹¹. If the gaps are of different widths, that is, $\Delta_{\text{tip}} \neq \Delta_{\text{sample}}$, we find peaks at $eV = \Delta_{\text{tip}} - \Delta_{\text{sample}}$ and $eV = -(\Delta_{\text{tip}} - \Delta_{\text{sample}})$. Throughout the experiment we used only tips that fulfilled $\Delta_{\text{tip}} = \Delta_{\text{sample}} = \Delta$. The superconducting state of the tip leads to an increase in energy resolution beyond the intrinsic Fermi–Dirac broadening of a normal metal tip¹¹, because the substrate's density of states is sampled with the sharp quasi-particle peaks of the tip.

Fe–OEP–Cl was sublimated from a crucible at 490 K onto the clean Pb(111) surface held at 120 K. To enhance self-assembly into ordered domains, the sample was subsequently annealed at 240 K for 180 s, before cooling down and transferring into the STM. Ordered monolayer islands of quasi-hexagonal structure can be identified, with the ethyl-groups clearly visible in the STM images (Fig. 1a). About 30% of the molecules show a bright protrusion in their centre. Annealing to higher temperatures after deposition reduces the number of protrusions. We can thus identify the protrusion as the central Cl ligand which is present when the molecules are evaporated from the powder. We can exclude any impurities adsorbed from the background pressure by a series of different preparations. The fraction of chlorinated molecules does not depend on the time for which the prepared sample is kept in the preparation chamber. The only observable influence is an elevated annealing temperature after molecule deposition. Reference 13 reports complete dechlorination during adsorption on thin Ni and Co layers at 300 K, whereas Fe–OEP–Cl deposited on Au(111) at 240 K retains the Cl ligand almost completely¹⁵. We focus our study on the molecules retaining their central chlorine ligand.

For the analysis of the excitation lifetime, A_{r1} and A_{r2} are quantified as the relative amplitude of the peaks appearing at the two inelastic onsets with respect to the amplitude of the BCS peak. They are defined as the ratio of the amplitudes of the inelastic peak and the BCS peak in the dI/dV spectra: $A_{r1} = A_1/A_{\text{BCS}}$ and $A_{r2} = A_2/A_{\text{BCS}}$, for the first and second excitations, respectively. Owing to the peaked nature of the superconducting density of states, this corresponds to the commonly employed measure of the increase of the differential conductance at the threshold of the excitation. A_1 (A_2), and A_{BCS} are determined as the mean amplitudes of the positive and negative bias sides of the first (second) excitation and of the BCS peak. For details see the Supplementary Information.

Received 28 March 2013; accepted 30 September 2013;
published online 10 November 2013

References

- Balashov, T. *et al.* Magnetic anisotropy and magnetization dynamics of individual atoms and clusters of Fe and Co on Pt(111). *Phys. Rev. Lett.* **102**, 257203 (2009).
- Khajetoorians, A. A. *et al.* Itinerant nature of atom-magnetization excitation by tunneling electrons. *Phys. Rev. Lett.* **106**, 037205 (2011).
- Kahle, S. *et al.* The quantum magnetism of individual Manganese-12-acetate molecular magnets anchored at surfaces. *Nano Lett.* **12**, 518–521 (2012).
- Loth, S., Eitzkorn, M., Lutz, C. P., Eigler, D. M. & Heinrich, A. J. Measurement of fast electron spin relaxation times with atomic resolution. *Science* **329**, 1628–1630 (2010).
- Loth, S. *et al.* Controlling the state of quantum spins with electric currents. *Nature Phys.* **6**, 340–344 (2010).
- Heinrich, A. J., Gupta, J. A., Lutz, C. P. & Eigler, D. M. Single-atom spin-flip spectroscopy. *Science* **306**, 466–469 (2004).
- Tsukahara, N. *et al.* Adsorption-induced switching of magnetic anisotropy in a single iron(II) phthalocyanine molecule on an oxidized Cu(110) surface. *Phys. Rev. Lett.* **102**, 167203 (2009).
- Shiba, H. Classical spins in superconductors. *Prog. Theor. Phys.* **40**, 435–451 (1968).
- Yazdani, A., Jones, B. A., Lutz, C. P., Crommie, M. F. & Eigler, D. M. Probing the local effects of magnetic impurities on superconductivity. *Science* **275**, 1767–1770 (1997).
- Ji, S.-H. *et al.* High-resolution scanning tunneling spectroscopy of magnetic impurity induced bound states in the superconducting gap of Pb thin films. *Phys. Rev. Lett.* **100**, 226801 (2008).
- Franke, K. J., Schulze, G. & Pascual, J. I. Competition of superconducting phenomena and Kondo screening at the nanoscale. *Science* **332**, 940–944 (2011).
- Gatteschi, D., Sessoli, R. & Villain, J. *Molecular Nanomagnets* (Oxford Univ. Press, 2006).
- Wende, H. *et al.* Substrate-induced magnetic ordering and switching of iron porphyrin molecules. *Nature Mater.* **6**, 516–520 (2007).
- Nishio, T. *et al.* Ground-state high-spin iron (III) octaethylporphyrin as studied by single-crystal cw/pulsed ESR spectroscopy. *Synth. Met.* **121**, 1820–1821 (2001).
- Heinrich, B. W. *et al.* Change of the magnetic coupling of a metal–organic complex with the substrate by a stepwise ligand reaction. *Nano Lett.* **13**, 4840–4843 (2013).
- Jaklevic, R. C. & Lambe, J. Molecular vibration spectra by electron tunneling. *Phys. Rev. Lett.* **17**, 1139–1140 (1966).
- Stipe, B. C., Rezaei, M. A. & Ho, W. Single-molecule vibrational spectroscopy and microscopy. *Science* **280**, 1732–1735 (1998).
- Hirjibehedin, C. F., Lutz, C. P. & Heinrich, A. J. Spin coupling in engineered atomic structures. *Science* **312**, 1021–1024 (2006).
- Hirjibehedin, C. F. *et al.* Large magnetic anisotropy of a single atomic spin embedded in a surface molecular network. *Science* **317**, 1199–1203 (2007).
- Chilian, B. *et al.* Anomalously large g factor of single atoms adsorbed on a metal substrate. *Phys. Rev. B* **84**, 212401 (2011).
- Leuenberger, M. N. & Loss, D. Spin relaxation in Mn₁₂-acetate. *Europhys. Lett.* **46**, 692–698 (1999).
- Ternes, M. *et al.* Interplay of conductance, force, and structural change in metallic point contacts. *Phys. Rev. Lett.* **106**, 016802 (2011).
- Parks, J. J. *et al.* Mechanical control of spin states in spin-1 molecules and the underscreened Kondo effect. *Science* **328**, 1370–1373 (2010).
- Leuenberger, M. N. & Loss, D. Quantum computing in molecular magnets. *Nature* **410**, 789–793 (2001).

Acknowledgements

We thank P. Brouwer, F. von Oppen, N. Lorente and M. Ternes for fruitful discussions. Financial support by the Deutsche Forschungsgemeinschaft through Sfb 658 and by the focus area Nanoscale of Freie Universität Berlin is gratefully acknowledged.

Author contributions

B.W.H., J.I.P. and K.J.F. designed the experiments. B.W.H. and L.B. performed the experiment. All authors discussed the data analysis and the results. B.W.H., J.I.P. and K.J.F. co-wrote the paper.

Additional information

Supplementary information is available in the online version of the paper. Reprints and permissions information is available online at www.nature.com/reprints. Correspondence and requests for materials should be addressed to B.W.H.

Competing financial interests

The authors declare no competing financial interests.